

Supporting information

Mechanistic Understanding of Tungsten Oxide In-Plane Nanostructure Growth via Sequential Infiltration Synthesis

Jae Jin Kim,[†] Hyo Seon Suh,[‡] Chun Zhou,[‡] Anil U. Mane,[§] Byeongdu Lee,[†] Soojeong Kim,[†] Jonathan D. Emery,^{||} Jeffrey W. Elam,[§] Paul F. Nealey,[‡] Paul Fenter,[†] Timothy T. Fister*,[†]

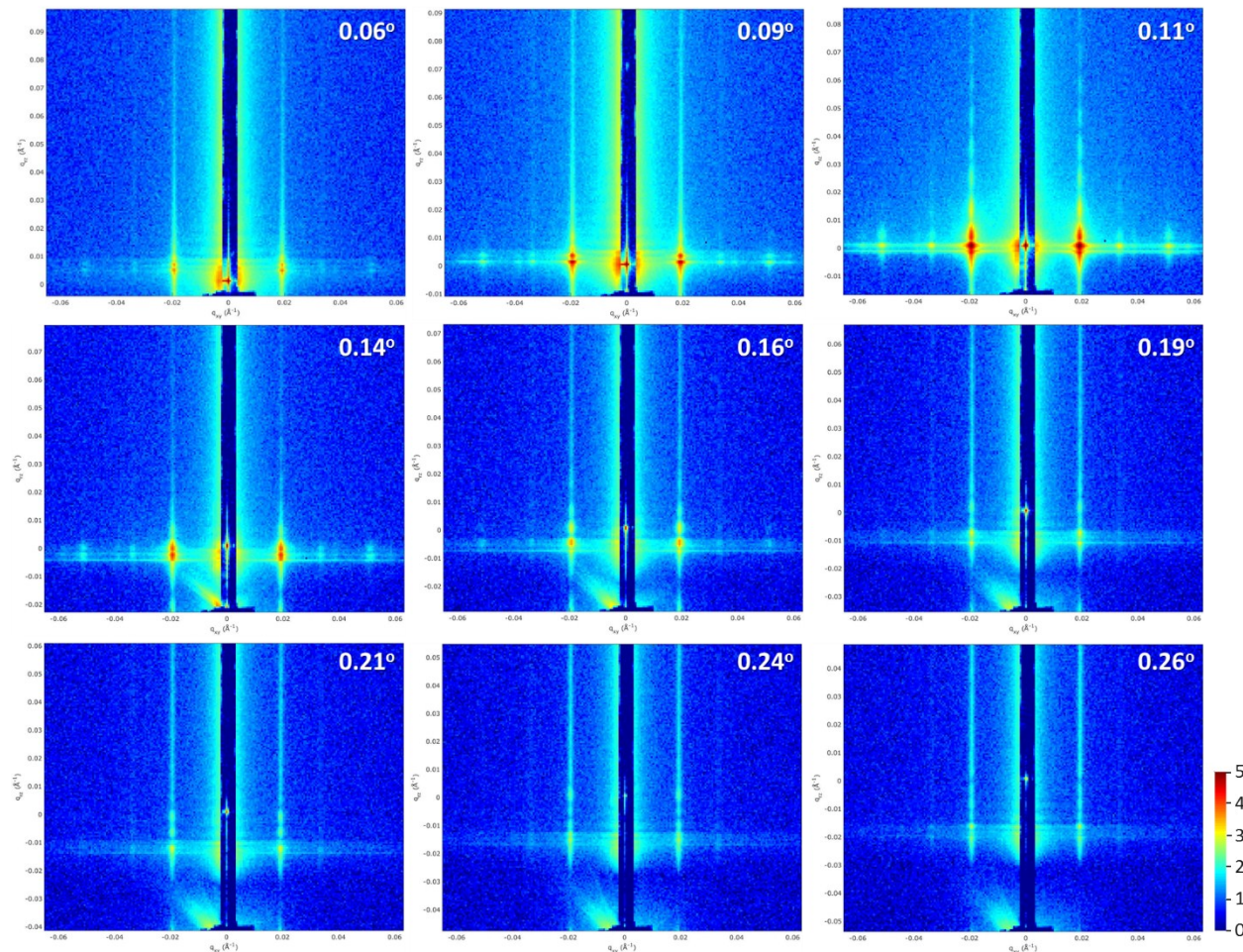


Figure S1 Grazing-incidence small-angle X-ray scattering (GISAXS) patterns from as-prepared self-assembled block copolymer (BCP) film of poly(styrene-*b*-methyl methacrylate (PS-*b*-PMMA) with $M_n = 46k/21k$ used as a template. The incident angle (α_i) of X-ray beam against the films was scanned from 0.06° to 0.26° as shown in the inset. The x and y axes are q_{xy} and $q_{r,z}$, respectively.

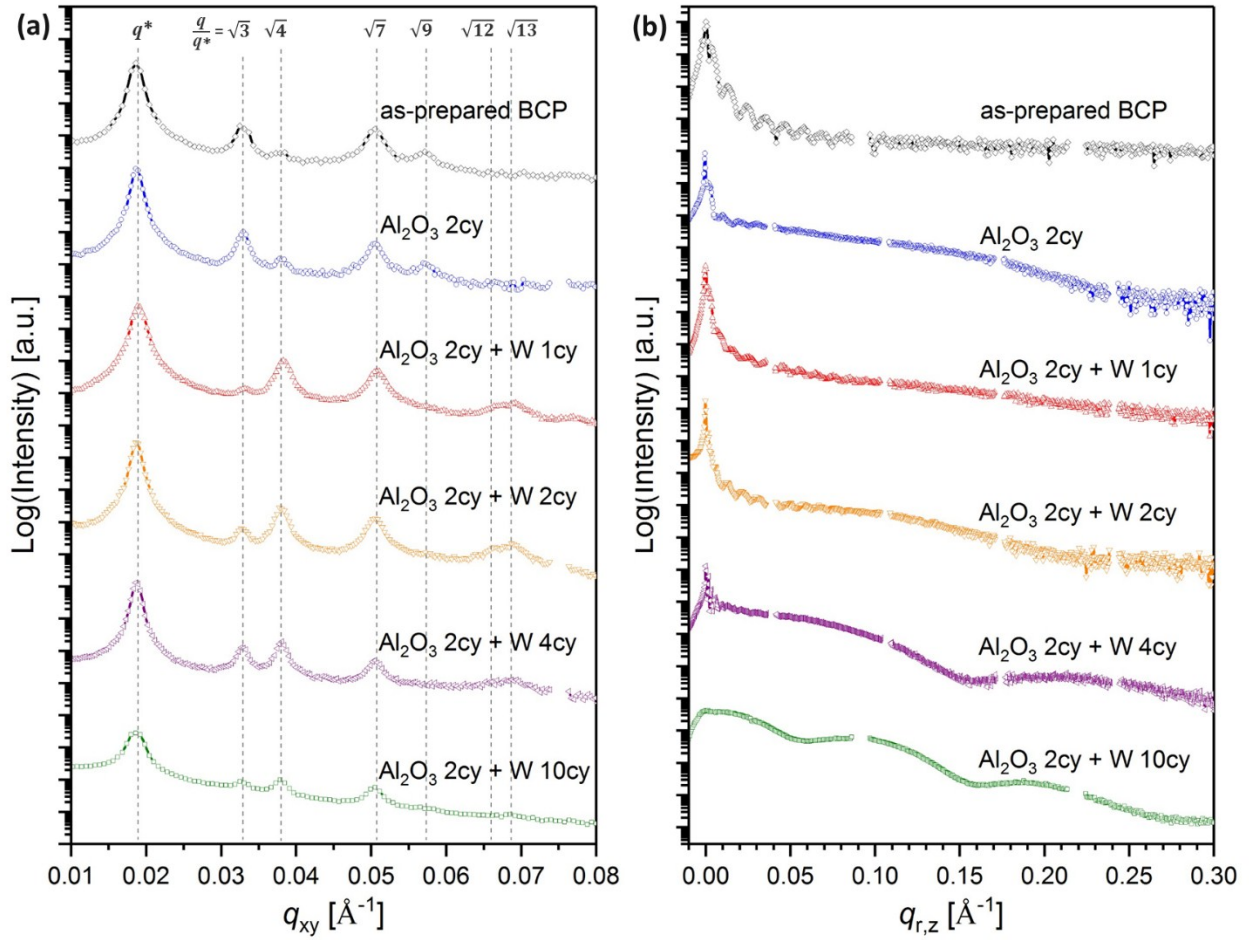


Figure S2 (a) In-plane and (b) out-of-plane line profiles of GISAXS data (displayed at Figure 2 in the main text) for as-prepared BCP film and samples after sequential infiltration synthesis (SIS) of Al_2O_3 seed (2 cycles) and subsequent W SIS deposition (1, 2, 4 and 10 cycles). The incident angles (α_i) of the X-ray beam with respect to the film surface plane were $0.10^\circ - 0.11^\circ$ as indicated at Figure 2 in the main text. In-plane and out-of-plane line profiles were extracted along the q_{xy} direction near the reflected direct beam and the $q_{r,z}$ direction at the primary diffraction peak, respectively. Self-assembled BCP film of PS-*b*-PMMA with $M_n = 46\text{k}/21\text{k}$ was used as a template.

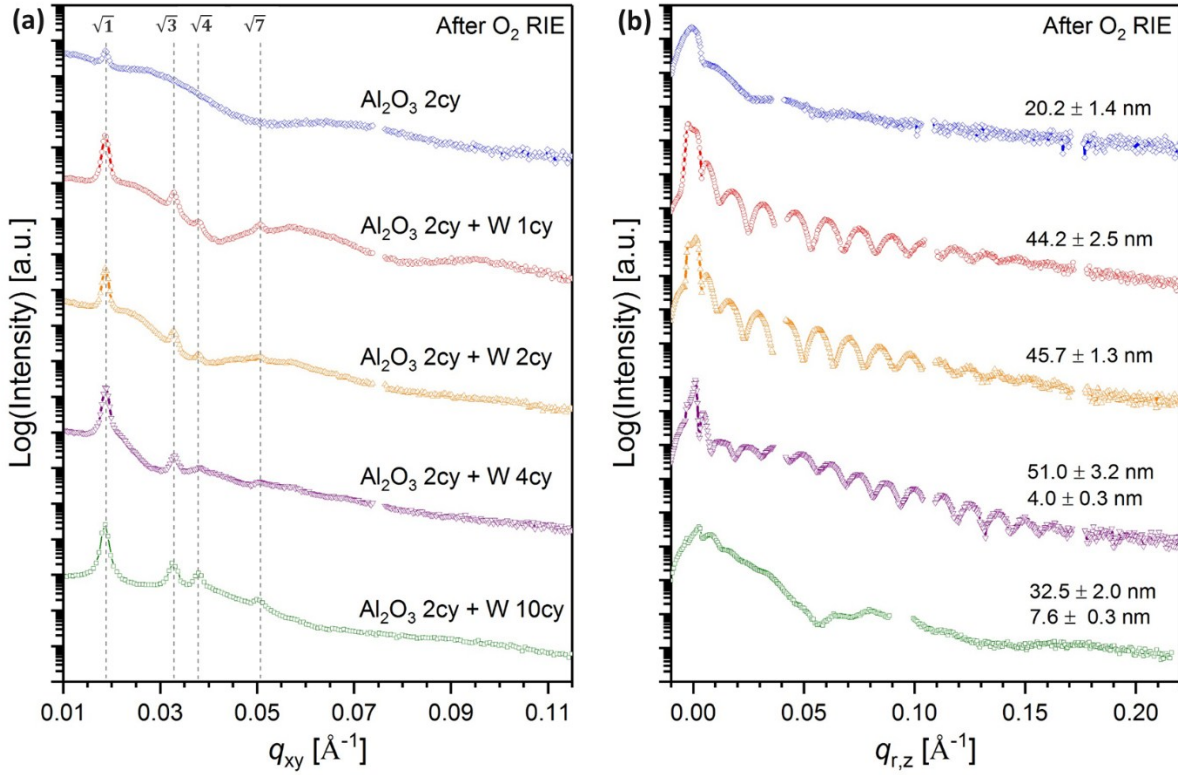


Figure S3 (a) In-plane and (b) out-of-plane line profiles of GISAXS data (displayed at Figure 3) for nanostructured samples after Al_2O_3 seed SIS (2 cycles) and following W SIS deposition (1, 2, 4 and 10 cycles) and subsequent O_2 reactive ion etching (RIE). The incident angles (α_i) of X-ray beam against the films were $0.09^\circ - 0.10^\circ$. In-plane and out-of-plane line profiles were extracted along the q_{xy} direction near the reflected direct beam and the $q_{r,z}$ direction at the primary diffraction peak, respectively. The film thicknesses extracted from out-of-plane line profiles are listed in (b). Self-assembled BCP film of $\text{PS-}b\text{-PMMA}$ with $M_n = 46\text{k}/21\text{k}$ was used as a template.

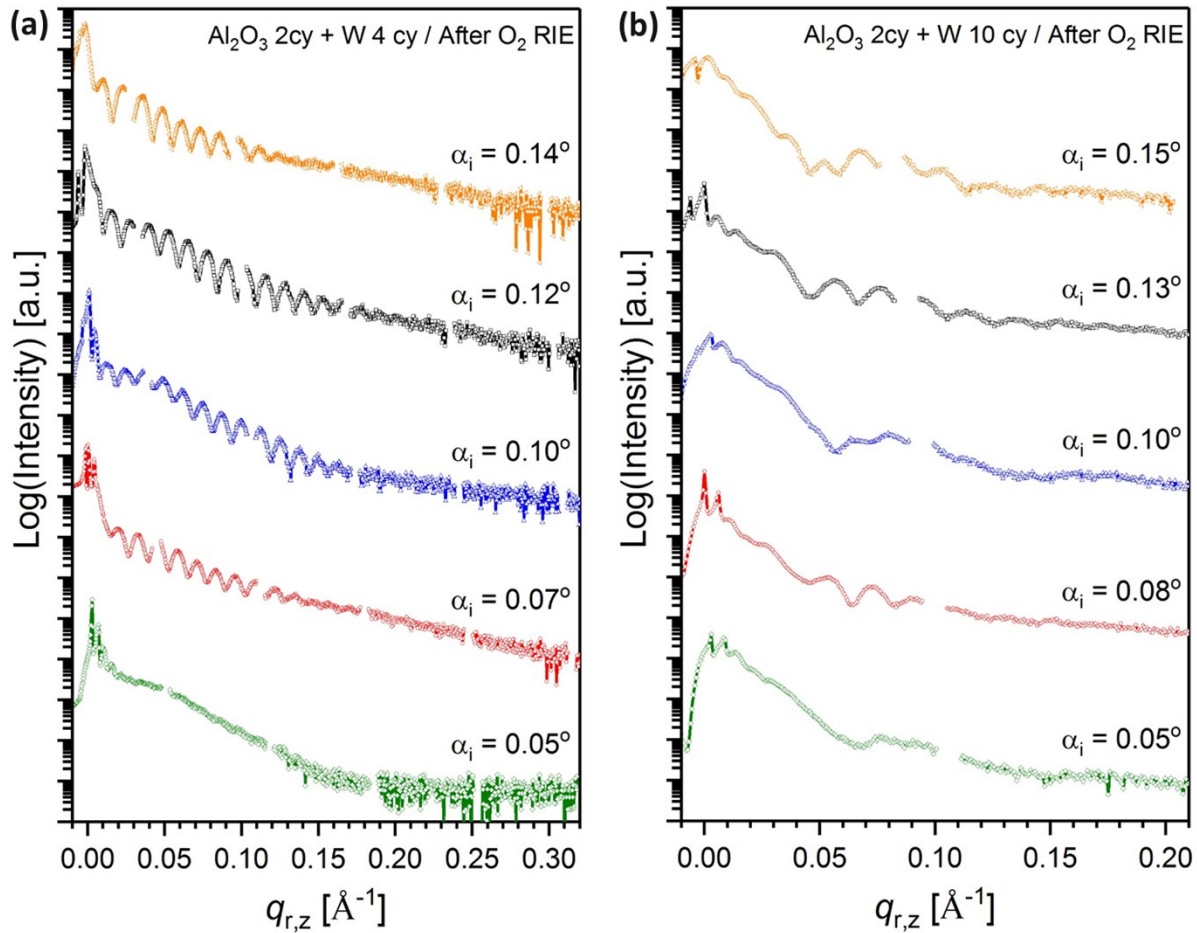


Figure S4 Out-of-plane line profiles of GISAXS data for nanostructured samples after Al_2O_3 seed SIS (2 cycles), then W SIS (a) 4 cycles and (b) 10 cycles, and subsequent O_2 RIE. The incident angle (α_i) of X-ray beam against the films was scanned from 0.05° to 0.15° . Profiles were extracted along the $q_{r,z}$ direction at the primary diffraction peak. Self-assembled BCP film of PS-*b*-PMMA with $M_n = 46\text{k}/21\text{k}$ was used as a template.

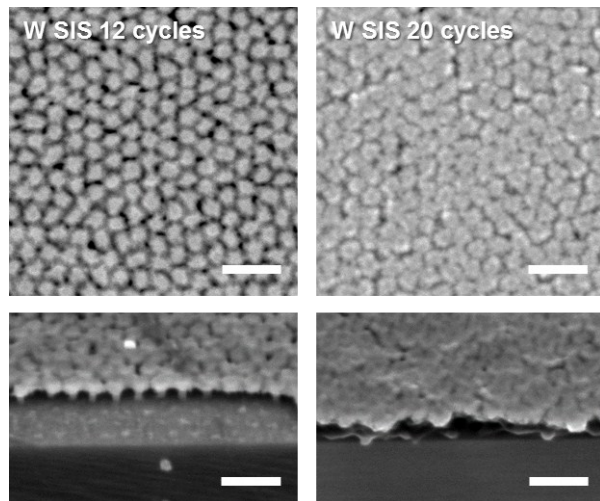


Figure S5 Plan-view / cross-sectional Scanning electron microscopy images of the samples prepared by Al_2O_3 SIS 2 cycles and W SIS 12 and 20 cycles and subsequent O_2 RIE, respectively. The inset scale bars indicate 100 nm. Self-assembled BCP film of $\text{PS-}b\text{-PMMA}$ with $M_n = 46\text{k}/21\text{k}$ was used as a template.

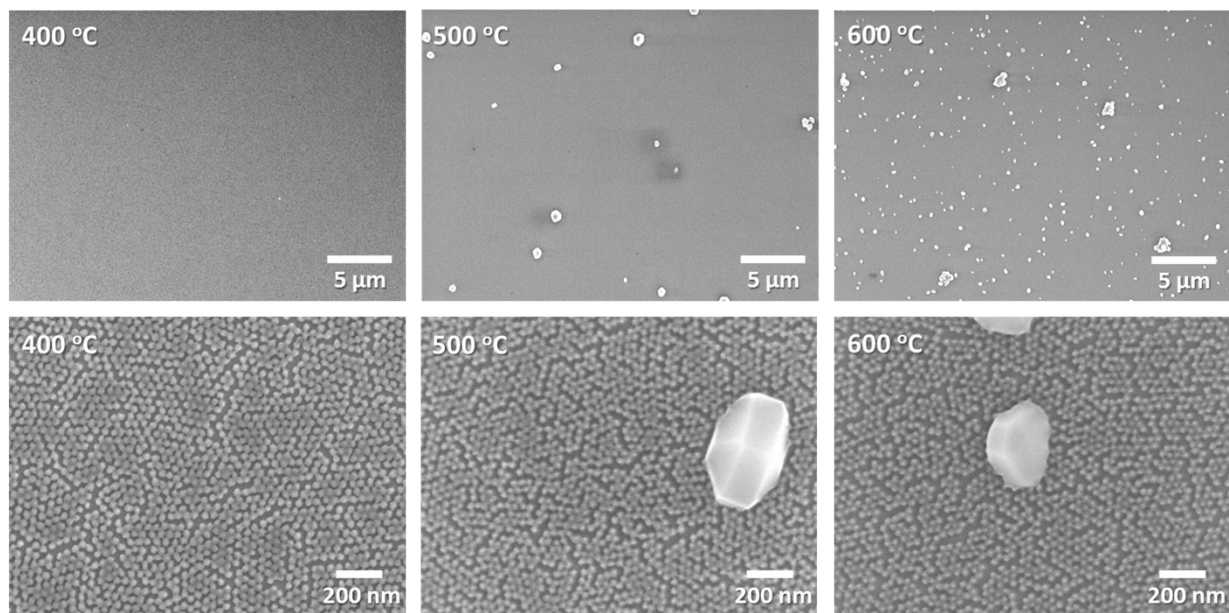


Figure S6 Scanning electron microscopy (SEM) images of the samples prepared by Al_2O_3 SIS 2 cycles and W SIS 10 cycles and subsequent O_2 RIE, then lastly annealed at 400 °C, 500 °C and 600 °C in air for 3 hours, respectively. Self-assembled BCP film of $\text{PS-}b\text{-PMMA}$ with $M_n = 46\text{k}/21\text{k}$ was used as a template.